Available online at www.sciencedirect.com
ScienceDirect
Polymer 48 (2007) 7241–7248
polymer
www.elsevier.com/locate/polymer

Emulsifier-free core–shell polyacrylate latex nanoparticles containing fluorine and silicon in shell

Xuejun Cui [a], Shuangling Zhong [b], Hongyan Wang [a,*]

[a] Department of Chemistry, Jilin University, Changchun 130012, People's Republic of China
[b] Alan G MacDiarmid Institute, Department of Chemistry, Jilin University, Changchun 130012, People's Republic of China

Received 24 July 2007; received in revised form 12 October 2007; accepted 17 October 2007
Available online 23 October 2007

Abstract

The emulsifier-free core–shell polyacrylate latex nanoparticles containing fluorine and silicon in shell were successfully synthesized by emulsifier-free seeded emulsion polymerization with water as the reaction medium. The silicon-containing fluorinated polymer could be fixed on the surface of polyacrylate nanoparticles due to the formation of the crosslinked network structure. Transmission electron microscopy (TEM) and dynamic light scattering (DLS) analysis indicated that the obtained emulsifier-free core–shell nanoparticles were uniform and possessed narrow size distributions. The core–shell structure and chemical components of the emulsifier-free core–shell nanoparticles were investigated by TEM and Fourier transform infrared (FTIR) spectrometry, respectively. X-ray photoelectron spectroscopy (XPS) analysis and contact angle measurement on the latex films proved the propensity of fluorine and silicon enrichment at film–air interface. In addition, the thermal stability of the latex films was improved with increasing the concentration of fluorine and silicon.

Keywords: Emulsifier-free; Core–shell; Silicon-containing fluorinated polyacrylate

1. Introduction

Both fluorinated and silicon-containing polymers have attracted increasing interest and been widely used in automotive and aerospace industries, optics and microelectronics. Fluorinated polymers have many desirable advantages including unique surface and optical properties, high thermal, chemical and weather resistance owing to the low polarizability and the strong electronegativity of fluorine atom [1–6]. Among numerous fluorinated polymers, fluorinated acrylic polymers with perfluoroalkyl groups have shown extraordinary characteristics: the pendant $-CF_3$ end groups on the perfluoroalkyl groups provide the polymers with extremely low surface energies and the acrylic groups ensure that the polymers can adhere well to various substrates [2,7]. Therefore, fluorinated acrylic polymers have attracted a great deal of attention of many researchers due to their unique properties and promising applications [3,5,8–10].

Surface properties of materials have significant effect on the integrated performance of materials and are usually predominated by the architecture and chemical components of the outermost surface layer. In order to obtain good surface properties, the surface of fluorinated acrylic polymers should be covered by as many perfluoroalkyl groups as possible. One possible strategy to achieve this purpose is to prepare the polyacrylate particles consisting of fluorine-free core and fluorinated shell [11–16], which can not only keep the excellent physical and chemical properties of materials but also decrease the expense of manufacturing fluorine-containing materials.

Core–shell fluorinated polyacrylate particles are usually produced by emulsion polymerization or miniemulsion polymerization. However, the residual emulsifier in latexes would have negative effects on the purification and the properties of the products and induce the environmental pollution. To avoid

* Corresponding author. Tel.: +86 431 85168470; fax: +86 431 85175863.
E-mail address: wang_hy@jlu.edu.cn (H. Wang).

0032-3861/$ - see front matter © 2007 Elsevier Ltd. All rights reserved.
doi:10.1016/j.polymer.2007.10.019

the drawbacks resulted from emulsifier, the investigations on developing emulsifier-free latexes have been made by some researchers. Compared with the conventional emulsion polymerization, the emulsifier-free emulsion polymerization endows latexes with one or more of the following advantages [17,18]: no emulsifier migration during film formation, excellent shear stability and monodisperse particle size distribution. Consequently, emulsifier-free emulsion polymerization is a very promising method in preparing environment friendly fluorinated polyacrylate particles with excellent properties.

In addition, it is well known that the fluorinated groups have the tendency to migrate toward interface and preferentially locate at the interface to minimize the interfacial energy [19–25]. However, a dilemma is that the fluorinated groups may migrate to the inside of films and hence lead to the decrease of film properties when the environment surrounding the latex changes, for instance, by being immersed into the water [26]. If the fluorinated groups can be fixed on the surface of films, this problem might be resolved.

In present study, the core–shell polyacrylate latex nanoparticles containing fluorine and silicon in shell were successfully synthesized by emulsifier-free seeded emulsion polymerization of dodecafluoroheptyl methacrylate and vinyltriethoxysilicone with crosslinked polyacrylate nanoparticles as seeds in water. The incorporation of vinyltriethoxysilicone in shell offers two functions: one is that silicon-containing polymers can represent exceptionally low glass transition temperature, low elastic modulus, high thermal and chemical stability [27]; the other is that the hydrolysis and condensation of $Si(OR)_3$ groups in vinyltriethoxysilicone can construct a crosslinked silica network [28,29]. The formation of silica network can not only improve the stability and mechanical strength of films but also immobilize tightly the fluorinated polymer on the surface of particles, which are beneficial for representing the properties of fluorine and silicon [30–33]. Hence, it is expected that combining the unique properties of both fluorinated and silicon-containing polymers in a single polymer can provide an interesting new material with more outstanding performance. The resulting emulsifier-free core–shell polyacrylate latex nanoparticles containing fluorine and silicon in shell may be a promising and environment friendly candidate in widespread applications, such as biomaterials as well as chemical, electrical and mechanical fields.

The core–shell polyacrylate latex nanoparticles containing fluorine and silicon in shell were characterized by various methods in this paper, including transmission electron microscopy (TEM), dynamic light scattering (DLS) analysis, Fourier transform infrared (FTIR) spectrometry, X-ray photoelectron spectroscopy (XPS) and thermogravimetric analysis (TGA), etc.

2. Experimental section

2.1. Materials

Butyl acrylate (BA, 99+%, Aldrich) and methyl methacrylate (MMA, 99%, Aldrich) were distilled under a nitrogen atmosphere and reduced pressure prior to polymerization. Dodecafluoroheptyl methacrylate $CH_2{=}C(CH_3)COOCH_2CF(CF_3)CFHCF(CF_3)_2$ (2,4-di(trifluoromethyl)-2,3,4,5,5,5-hexafluoropentyl methacrylate, Actyflon-G04 or DFHMA) and vinyltriethoxysilicone (VTES) were, respectively, obtained from XEOGIA Fluorine–Silicon Chemical Co., Ltd. and Shanghai Huarun Chemical Company of China, and used as received. Triethylene glycol dimethacrylate (TrEGDMA) was used as crosslinking reagent without further purification. The monomers were stored at 5 °C. Ammonium persulfate (APS, Aldrich) and sodium bicarbonate ($NaHCO_3$) were used as received. The reactive emulsifier, 4-styrenesulfonic acid, sodium salt hydrate (NaSS, 99+%), was used as received from Aldrich. The water used in this experiment was distilled followed by deionization.

2.2. Emulsifier-free core–shell emulsion polymerization

The emulsifier-free core–shell polyacrylate latex nanoparticles containing fluorine and silicon in shell were synthesized by seeded emulsion polymerization technique. All the polymerizations were carried out under nitrogen atmosphere in a 250 ml four-neck flask equipped with reflux condenser, mechanical stirrer, dropping funnels and inlet for nitrogen gas and heated in the water bath.

The recipes for the synthesis of the emulsifier-free core–shell latex nanoparticles are listed in Table 1. The core–shell latex was synthesized by two-stage, namely, core and shell formation.

2.2.1. Synthesis of the emulsifier-free crosslinked polyacrylate seed latex particles

First, an appropriate amount of NaSS was introduced into the four-neck flask charged with 90 ml of deionized water. After complete dissolution of NaSS in water, the mixture of 5.6 g of MMA, 5.4 g of BA and 0.3 g of TrEGDMA was added into the flask. The flask was then placed in water bath at 75 °C with a stirring rate of 300 rpm. After additional 30 min equilibration time, the ammonium persulfate (APS) aqueous solution (0.15 g of APS was dissolved in 5 ml water) was dropped into the above flask in 1 h. Then the temperature was raised to 80 °C and maintained at this temperature for 2 h. Thus, the crosslinked polyacrylate seed latex particles were obtained. The conversion of the first stage was determined gravimetrically and is reported in Table 1.

2.2.2. Synthesis of the emulsifier-free core–shell polyacrylate latex nanoparticles containing fluorine and silicon in shell

According to Table 1, the shell monomers mixture of DFHMA, VTES and TrEGDMA in the dropping funnel was fed into the flask containing seed latex under starved-feed addition. Simultaneously, the APS aqueous solution (0.1 g of APS was dissolved in 5 ml water) in the dropping funnel was fed into the flask with an appropriate dropping rate to initiate the polymerization of shell monomers at 80 °C. When the shell monomers mixture and APS solution were completely fed, the temperature was maintained at 80 °C for another 5 h. The obtained latex was cooled to room temperature and

Table 1
Recipes and properties of the polyacrylate latexes

	C1	C2	C3	C4	C5	CS1	CS2	CS3	CS4	CS5
First stage (core)										
BA (g)	5.4	5.4	5.4	5.4	5.4	5.4	5.4	5.4	5.4	5.4
MMA (g)	5.6	5.6	5.6	5.6	5.6	5.6	5.6	5.6	5.6	5.6
TrEGDMA (g)	0.3	0.3	0.3	0.3	0.3	0.3	0.3	0.3	0.3	0.3
NaSS (g)	0.01	0.03	0.05	0.07	0.09	0.05	0.05	0.05	0.05	0.05
APS (g)	0.15	0.15	0.15	0.15	0.15	0.15	0.15	0.15	0.15	0.15
DI water (g)	95.0	95.0	95.0	95.0	95.0	95.0	95.0	95.0	95.0	95.0
Second stage (shell)										
DFHMA (g)						4.80	3.20	1.60	1.60	1.60
VTES (g)						0.92	0.92	0.92	1.84	2.76
TrEGDMA (g)						0.1	0.1	0.1	0.1	0.1
APS (g)						0.1	0.1	0.1	0.1	0.1
DI water (g)						5.0	5.0	5.0	5.0	5.0
Conversion (%)	98.35	97.25	98.60	97.72	96.73	95.5	96.2	95.9	96.1	95.2
Particle size (nm)	263.4	249.7	172.5	180.4	184.1	242.8	223.8	197.1	235.9	252.6
Polydispersity	0.005	0.005	0.011	0.014	0.005	0.047	0.066	0.031	0.004	0.084
Water CA (°)			84.2			105.6	105.2	96.5	98.4	97.8
IPA CA (°)						20.9	15.4	13.7	11.1	8.4

the total conversion of comonomers was determined gravimetrically via the solids content as summarized in Table 1. The $NaHCO_3$ was used to control the pH value of the obtained latex in the range of 6–7.

2.3. Measurements

Scanning electron microscopy (SEM) micrographs were taken with SHIMADZU SSX-550 at voltage of 15.0 kV. The latexes were diluted with deionized water, dropped onto silicon wafer and dried at room temperature.

The micrographs of the emulsifier-free core–shell polyacrylate latex nanoparticles were obtained using transmission electron microscopy (TEM) on a JEM-2000 EX transmission electron microscope with an acceleration voltage of 200 kV. The samples were stained with 2% phosphotungstic acid solution.

The particle sizes and their distribution of the emulsifier-free crosslinked polyacrylate seed latexes and emulsifier-free core–shell polyacrylate latex nanoparticles were measured by ZetaPALS dynamic light scattering (DLS) detector (BI-90Plus, Brookhaven Instruments Corporation, Holtsville, NY, 15 mW laser, incident beam = 660 nm) at 25 °C. The scattering angle was fixed at 90°. The samples were highly diluted ($C < 0.01$ wt.%) before testing to prevent multiple scattering.

Fourier transform infrared (FTIR) spectra of KBr powder-pressed pellets were recorded on a Nicolet Instruments Research Series 5PC Fourier Transform Infrared Spectrometer in the range from 4000 to 400 cm^{-1}.

The emulsifier-free core–shell polyacrylate latex films were prepared by coating the latex onto the clean surface of glass and drying in a vacuum oven at 70 °C for 6 h. The films were transparent and their thicknesses were about 50 μm.

X-ray photoelectron spectra (XPS) measurements of the emulsifier-free core–shell polyacrylate latex film were performed on an ESCALAB Mark II (England) with Al kα (X-ray) lamphouse. The compositions of film–air and film–glass surfaces were determined, respectively.

Static contact angles (CAs) of water and iso-propanol (IPA) on the emulsifier-free core–shell polyacrylate latex films were measured with a JC2000C2 contact angle goniometer (Shanghai Zhongchen Powereach Company, China) by the sessile drop method with a microsyringe at 25 °C. More than 10 contact angles were averaged to get a reliable value for each sample.

Thermogravimetric analysis (TGA) was performed with a Pyris 1TGA (Perkin Elmer) under the nitrogen atmosphere at a heating rate of 10 °C/min from 25 to 650 °C.

3. Results and discussion

3.1. Microstructure of the core–shell latex nanoparticles

The basic characteristics of the resulting latex particles are summarized in Table 1. It is clear from Table 1 that the average particle diameter of the crosslinked polyacrylate seeds measured by DLS first decreases and then increases slightly with the increment of the amount of reactive emulsifier NaSS. Small seed latex particles are of great benefit to limit secondary nucleation and encourage core–shell particles formation in seeded emulsion polymerization [34]. Therefore, the sample C3 was chosen as the seeds for preparing the core–shell polyacrylate latex nanoparticles containing fluorine and silicon in shell due to its minimum average particle diameter. SEM micrograph of the sample C3 is shown in Fig. 1.

The emulsifier-free seeded emulsion polymerization and starved-feed technology of shell monomers (DFHMA, VTES and TrEGDMA) were employed to prepare the core–shell particles. The starved-feed addition is highly favorable to form core–shell structure and prevent secondary nucleation of P(DFHMA–VTES–TrEGDMA) [7,13,34,35]. Furthermore, the respective crosslinking of the core and shell of the particles could restrict the penetration of the shell monomers into the core, which leads to the polymerization of shell monomers on the surface of core and the formation of stable core–shell structure particles.

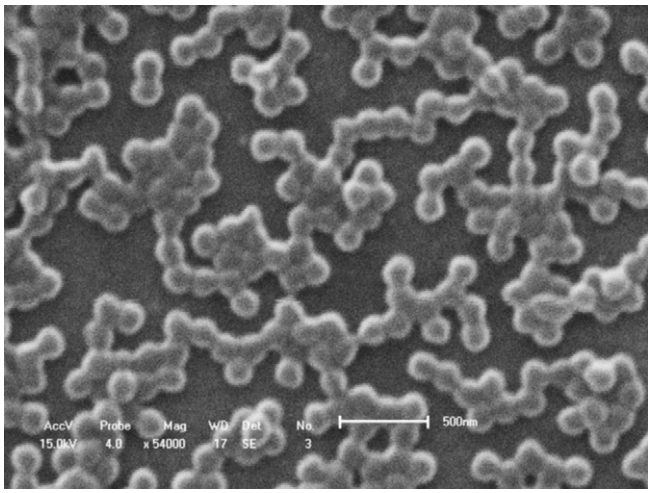

Fig. 1. SEM micrograph of the crosslinked polyacrylate seed particles (sample C3).

In order to confirm that DFHMA, VTES and TrEGDMA were indeed polymerized on the surface of the seed particles and formed the shell layer, TEM and DLS measurements were employed in this paper. Fig. 2 illustrates TEM micrographs of the representative emulsifier-free core–shell polyacrylate latex nanoparticles containing fluorine and silicon in shell. With careful staining of the particles using 2% phosphotungstic acid, a significant contrast between core and shell of the latex particles can be observed clearly in Fig. 2 as a result of the difference of electron penetrability to the core and shell, which evidently proves the formation of the core–shell structure. The light and dark regions in the particles correspond to crosslinked polyacrylate core and crosslinked silicon-containing fluorinated polyacrylate shell, respectively. Moreover, it is obvious from TEM micrographs that the dimensions of the shell layer increase with increasing the amount of shell monomers, which is consistent with the results of DLS analysis collected in Table 1. DLS measurements show that the average diameter of the seed particles (sample C3) is 172.5 nm, and the diameters of the core–shell silicon-containing fluorinated polyacrylate particles range from 197.1 to 252.6 nm as increasing the amount of shell monomers. Thus we could control the thickness of shell layer by varying the amount of shell monomers. Furthermore, DLS measurements exhibit that the polydispersity index of the polyacrylate seeds and the subsequent core–shell particles are all less than 0.1, indicating the monomodal distributions of resultant particles. The monomodal distributions and the growth in particle sizes of the core–shell latex particles suggest that no secondary nucleation occurs and the shell monomers polymerize quantitatively onto the surface of crosslinked polyacrylate seeds. According to the results of TEM and DLS, it can be concluded that the core–shell particles have been successfully obtained by emulsifier-free seeded emulsion polymerization method and the thickness of shell layer can be easily controlled by varying the amount of shell monomers.

3.2. FTIR spectra

The chemical structure of polyacrylate, core–shell polyacrylate containing fluorine in shell, core–shell polyacrylate containing silicon in shell and core–shell polyacrylate containing fluorine and silicon in shell were detected by FTIR and the results are presented in Fig. 3. All the polymers exhibit the characteristic stretching peaks of C–H (CH_2) at 2960 and 2875 cm^{-1}, stretching vibration of C=O at 1735 cm^{-1}, and distortion vibration of CH_2 at 1454 and 1390 cm^{-1}. Compared with the polyacrylate, the core–shell polyacrylate containing fluorine in shell exhibits the new peaks at about 1303, 689 and 617 cm^{-1} which are attributed to C–F stretching vibration and wagging vibration, and the core–shell polyacrylate containing silicon in shell also displays a new peak at about 1114 cm^{-1} which results from Si–O–Si asymmetric stretching vibration [36]. The appearance of Si–O–Si peak provides the evidence of hydrolysis and condensation reactions

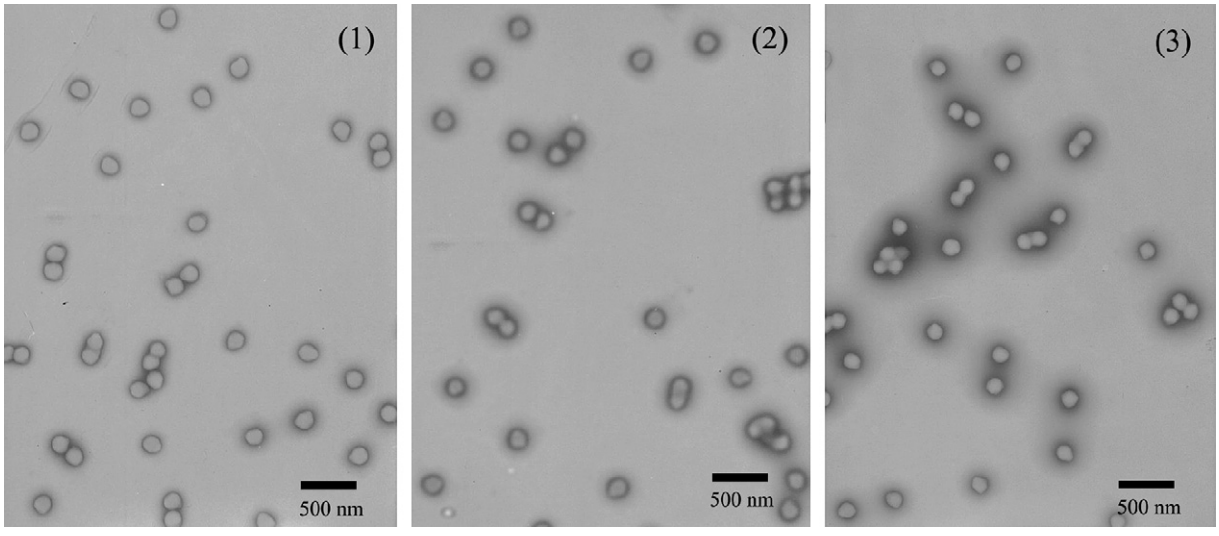

Fig. 2. TEM micrographs of the emulsifier-free core–shell polyacrylate latex nanoparticles containing fluorine and silicon in shell with different amount of DFHMA: (1) 1.60 g; (2) 3.20 g; and (3) 4.80 g.

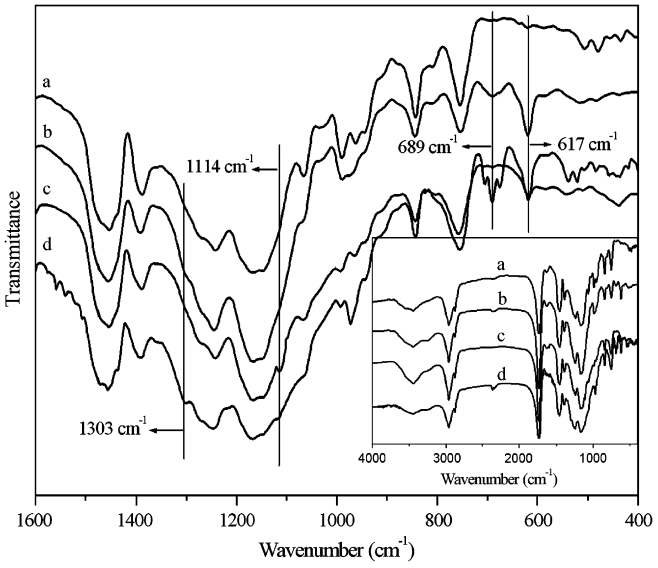

Fig. 3. FTIR spectra of emulsifier-free polyacrylate (a), emulsifier-free core–shell polyacrylate containing fluorine in shell (b), emulsifier-free core–shell polyacrylate containing silicon in shell (c) and emulsifier-free core–shell polyacrylate containing fluorine and silicon in shell (d).

(crosslinking) of $Si(OR)_3$ groups and suggests the formation of crosslinked silica network structure. All these new peaks can be detected in the FTIR spectrum of the core–shell polyacrylate containing fluorine and silicon in shell, indicating that fluorine and silicon have been successfully introduced onto the surface of polyacrylate seeds as desired through emulsifier-free seeded emulsion polymerization.

3.3. Surface analysis

XPS analysis can provide insights into the chemical compositions of polymer surface [15,16,26]. The chemical identification of the film–air and film–glass interfaces of core–shell polyacrylate containing fluorine and silicon in shell were also detected by XPS here. Take CS2 film for example, its XPS spectra reveal the strong characteristic signals of carbon, oxygen and fluorine as well as a weak silicon signal as expected (Fig. 4(1)). Discerning the chemical compositions of the F1s spectrum shows a singlet symmetrical peak (688.2 eV), the weak Si2p signal is visible at 102.5 eV while the O1s spectrum includes two peaks (534.5 and 535.7 eV) corresponding to the two different types of oxygen in the ester functional group of the acrylate polymers. The C1s spectrum, however, presents more complex pattern of peaks (284.3, 285.0, 286.9, 288.8 and 293.7 eV). The corresponding high resolution XPS spectra of C1s, F1s and Si2p peaks of CS2 film are also exhibited in Fig. 4. In the C1s window (Fig. 4(2)), the main peaks are attributed to the carbon atoms of C–Si groups, the aliphatic carbon atoms, the ester carbon atoms and the carbon atoms of CF and CF_3 groups, respectively. In the F1s window (Fig. 4(3)), it can be seen that the intensity of fluorine signal in the film–air interface is higher than that in the film–glass interface. The tendency of silicon signal (Fig. 4(4)) is the same as that of fluorine signal. These observations suggest that fluorine and silicon are preferentially located at the film–air interface. To further investigate these tendencies, the relative quantitative evaluation of XPS spectra were carried out by measuring the areas of C1s, O1s, F1s and Si2p peaks and multiplying them by the appropriate sensitivity factors. Table 2 summarizes the experimental values of elemental concentration percentages of C, O, F and Si elements on the topmost surface calculated from the survey scan and the theoretical ones calculated from the chemical formula of the monomer for the bulk. It can be observed from Table 2 that the CS2 film shows a remarkable enrichment of fluorine and silicon at the interface. That is, the experimental values of fluorine and silicon contents in the film–air interface are 32.86 and 2.78% which are about triplicity of the theoretical ones (11.74 and 0.88%) in the bulk. It can be understood based on the fact that fluorine and silicon atoms have extremely low surface free energy and self-aggregated property, which cause the fluorinated and silicon-containing segments to be preferentially oriented to the polymer surface during the film formation so as to decrease the surface energy of film [35,38]. Furthermore, both fluorine and silicon exhibit concentration gradient from the film–air interface to the film–glass interface. The experimental values of fluorine and silicon contents in the film–air interface are 36.57 and 14.88% higher than those in the film–glass interface, respectively. The XPS results are consistent with those reported in the literatures [15,16,26,37,39,40]. It is expected that the surface compositions have a significant influence on the hydrophobic property of the films, which will be discussed in the following paragraph.

The hydrophobic property of a polymeric material can be estimated in terms of contact angle measurement by depositing a water drop on the surface of film and the value of contact angle depends on the chemical compositions of film surface [7,30]. The higher the wetting resistance of film surface, the higher contact angle is. Because both fluorinated and silicon-containing polymers have good hydrophobic property and fluorine and silicon atoms tend to locate on the film surface during the film formation as mentioned before, it is expected that combining the fluorinated and silicon-containing monomers in a single polymer can increase the hydrophobic property of polymer. The contact angles of polyacrylate core precursor and emulsifier-free core–shell polyacrylate with various fluorine and silicon contents are shown in Table 1. One can see that when the fluorinated and silicon-containing monomers are introduced into the polymer chains of shell, the core–shell silicon-containing fluorinated polyacrylate latex films show higher contact angle compared with the polyacrylate core without fluorine and silicon as expected. In addition, in the case of fixing VTES content (silicon content), the contact angles of the emulsifier-free core–shell silicon-containing fluorinated polyacrylate latex films increase from 96.5 to 105.2° as the DFHMA content in the shell increases from 1.60 to 3.20 g due to the increment of hydrophobic fluorine content. Then the incremental tendency of contact angle begins to weaken at the higher fluorine content, indicating that the fluorine enriched on film surface has tended to reach a maximum and hence further increasing DFHMA content has only little influence on

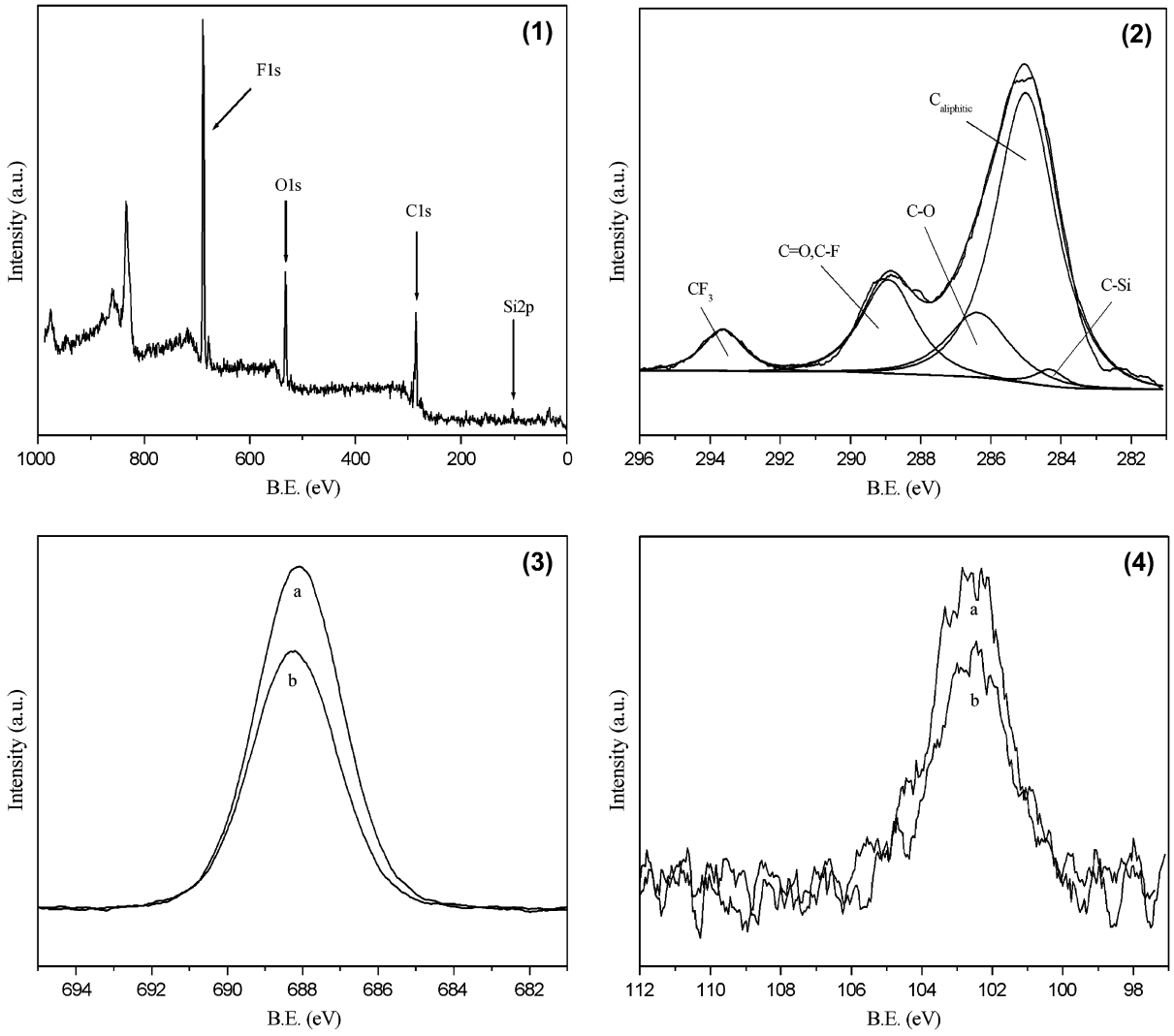

Fig. 4. XPS spectra of the film of emulsifier-free core–shell polyacrylate containing fluorine and silicon in shell (sample CS2): (1) wide scanning spectra for the film–air interface, (2) deconvolution of C1s signals for the film–air interface, (3) F1s signals for the film–air interface (a) and the film–glass interface (b), and (4) Si2p signals for the film–air interface (a) and the film–glass interface (b).

the hydrophobic property of core–shell particles [13]. In the case of fixing DFHMA content (fluorine content), the contact angles of core–shell silicon-containing fluorinated polyacrylate latex films first increase and then decrease with increment of VTES content, as shown in Table 1. It is because that after incorporating VTES into the shell, the hydrolysis and condensation of $Si(OR)_3$ groups can construct a crosslinked silica network. The formation of silica network can inhibit water entering the films and hence increase the water contact angle. However, the compressive network will hinder more hydrophobic perfluoroalkyl groups orientating to film–air interface when the VTES content reaches to an extent (2.76 g), which leads to the decrease in the water contact angle. Furthermore, the iso-propanol (IPA) contact angles are also measured on the polyacrylate latex films and shown in Table 1. The IPA contact angles decreased from 13.7 to 8.4° indicating the decreasing of the fluorine content on surface with increasing silicon content. The contact angle measurements also indicate that the polyacrylate cores have been enwrapped by the fluorinated and silicon-containing polymer shell as desired.

Table 2
Element contents of the film interfaces of emulsifier-free core–shell polyacrylate containing fluorine and silicon in shell (sample CS2)

Item	Element	Peak area	Sensitivity factor	Determined (%)	Theoretical (%)
Film–air interface	C1s	13,454	0.25	45.29	55.77
	O1s	14,938	0.66	19.05	24.40
	F1s	39,038	1.0	32.86	11.74
	Si2p	898	0.27	2.78	0.88
Film–glass interface	C1s	15,422	0.25	51.53	55.77
	O1s	17,369	0.66	21.98	24.40
	F1s	28,803	1.0	24.06	11.74
	Si2p	783	0.27	2.42	0.88

3.4. Thermal stability

TGA was used to investigate the thermal stability of the core–shell silicon-containing fluorinated polyacrylate films

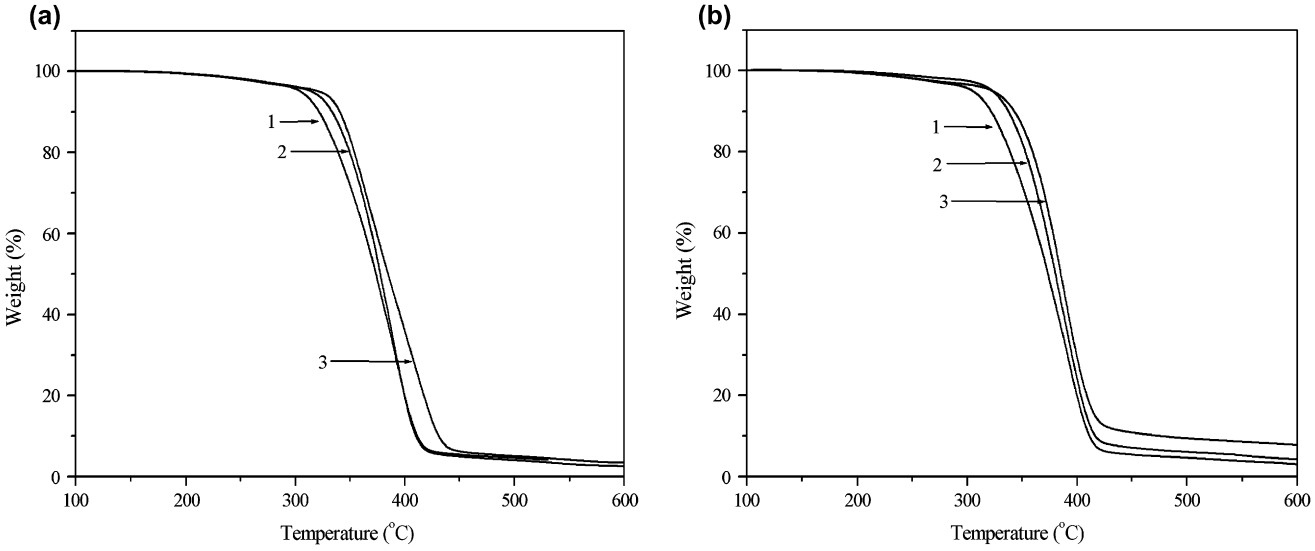

Fig. 5. The TGA curves of the emulsifier-free core–shell polyacrylate containing fluorine and silicon in shell: (a) with different amounts of DFHMA 1: 1.60 g (CS3), 2: 3.20 g (CS2), 3: 4.80 g (CS1); and (b) with different amounts of VTES 1: 0.92 g (CS3), 2: 1.84 g (CS4), 3: 2.76 g (CS5).

and the results are depicted in Fig. 5. It can be seen from Fig. 5(a) that the weight loss of core–shell silicon-containing fluorinated polyacrylate CS3 begins at around 314 °C which is attributed to the decomposition of main chain. When increasing the DFHMA content from 1.6 to 4.8 g, the decomposition temperature increases from 314 to 338 °C, indicating that the thermal stability of latex film is improved with the increment of fluorine content. It is because that through emulsifier-free seeded emulsion polymerization, the fluorinated polyacrylate concentrates in the shell of the latex particles and hence the perfluoroalkyl groups containing C–F bond with high bond energy can shield and protect the non-fluorinated segment beneath them. Thus the thermal stability of core–shell silicon-containing fluorinated polyacrylate is improved due to the increment of C–F bond in the shell by increasing the amount of DFHMA. In addition, the thermal stability of latex films can also be improved by increasing VTES content as shown in Fig. 5(b). On the one hand, the hydrolysis and condensation of $Si(OR)_3$ groups can construct a crosslinked silica network. The crosslinked network makes the shell more compact and can immobilize the fluorinated copolymer tightly in the shell. On the other hand, the silica itself is temperature tolerant. Both effects can improve the thermal stability of latex films, hence the decomposition temperature of latex films elevates with the increment of VTES concentration. It can be concluded from Fig. 5 that the thermal stability of silicon-containing fluorinated polyacrylate films can be improved by increasing the amount of DFHMA and VTES introduced into the shell, respectively.

4. Conclusion

The uniform emulsifier-free core–shell polyacrylate latex nanoparticles containing fluorine and silicon in shell were successfully synthesized by emulsifier-free seeded emulsion polymerization of fluorinated methacrylate and vinyltriethoxysilicone surrounding crosslinked polyacrylate core with water as the reaction medium. TEM micrographs revealed that the polyacrylate core had been surrounded by the silicon-containing fluorinated polymer shell. The silicon-containing fluorinated polymer shell could be stably fixed on the surface of polyacrylate core due to the formation of the crosslinked polymer network. The particle sizes of the core–shell latexes increased with increasing the amount of shell monomers, which is consistent with the results of DLS measurements. XPS analyses indicated that the fluorine and silicon preferentially located at the surface of latex films. Compared with the polyacrylate seed latex film, the core–shell silicon-containing fluorinated polyacrylate latex films exhibited higher water contact angles, indicating they possessed higher hydrophobic property. Furthermore, the thermal stability of emulsifier-free core–shell silicon-containing fluorinated polyacrylate latex film was improved with increasing the concentration of fluorine and silicon, respectively. The emulsifier-free seeded emulsion polymerization is a potentially promising method in preparing environment friendly core–shell silicon-containing fluorinated polyacrylate nanoparticles.

Acknowledgement

This work was supported by the National Science Foundation of China (Grant nos. 50573027 and 50673032).

References

[1] van Ravenstein L, Ming W, van de Grampel RD, van der Linde R, de With G, Loontjens T, et al. Macromolecules 2004;37(2):408–13.
[2] Park IJ, Lee SB, Choi CK. Polymer 1997;38:2523–7.
[3] Ameduri B, Bongiovanni R, Malucelli G, Pollicino A, Priola A. J Polym Sci Part A Polym Chem 1999;37:77–87.
[4] Pomes V, Fernandez A, Costarramone N, Grano B, Houi D. Colloid Surf A 1999;159(2–3):481–90.
[5] Yang S, Wang J, Ogino K, Valiyaveettil S, Ober CK. Chem Mater 2000;12:33–40.

[6] Lee JR, Jin FL, Park SJ, Park JM. Surf Coat Technol 2004;180–181: 650–4.
[7] Ha JW, Park IJ, Lee SB. Macromolecules 2005;38:736–44.
[8] Sacher E. Prog Surf Sci 1994;47:273–300.
[9] Pu FR, Williams RL, Markkula TK, Hunt JA. Biomaterials 2002;23: 2411–28.
[10] Lazzari M, Chiantore O, Castelvetro V. Polym Int 2001;50:863–8.
[11] Landfester K, Rothe R, Antonietti M. Macromolecules 2002;35: 1658–62.
[12] Cheng SY, Chen YJ, Chen ZG. J Appl Polym Sci 2002;85:1147–53.
[13] Ha JW, Park IJ, Lee SB, Kim DK. Macromolecules 2002;35:6811–8.
[14] Marion P, Beinert G, Juhué D, Lang J. Macromolecules 1997;30:123–9.
[15] Marion P, Beinert G, Juhué D, Lang J. J Appl Polym Sci 1997;64: 2409–19.
[16] Zhang CC, Chen YJ. Polym Int 2005;54:1027–33.
[17] Ohtsuka Y, Kawaguchi H, Sugi Y. J Appl Polym Sci 1981;26:1637–47.
[18] Ceska GW. J Appl Polym Sci 1974;18:427–37.
[19] Sun F, Castner DG, Mao G, Wang W, McKeown P, Grainger DW. J Am Chem Soc 1996;118:1856–66.
[20] Iyengar DR, Perutz SM, Dai C, Ober CK, Kramer EJ. Macromolecules 1996;29:1229–34.
[21] Thomas RR, Anton DR, Graham WF, Darmon MJ, Sauer BB, Stika KM, et al. Macromolecules 1997;30:2883–90.
[22] Anton D. Adv Mater 1998;10:1197–205.
[23] Thomas RR, Anton DR, Graham WF, Darmon MJ, Stika KM. Macromolecules 1998;31:4595–604.
[24] Thomas RR, Glaspey DF, DuBois DC, Kirchner JR, Anton DR, Lloyd KG, et al. Langmuir 2000;16:6898–905.
[25] Xiang M, Li X, Ober CK, Char K, Genzer J, Sivaniah E, et al. Macromolecules 2000;33:6106–19.
[26] Schmidt DL, Brady RF, Lam K, Schmidt DC, Chaudhury MK. Langmuir 2004;20:2830–6.
[27] Brinker CJ, Scherer GW. Sol–gel science: the physics and chemistry of sol–gel processing. Boston: Academic Press; 1990.
[28] Marcu I, Daniels ES, Dimonie VL, Hagiopol C, Roberts JE, El-Aasser MS. Macromolecules 2003;36:328–32.
[29] Ren SZ, Sun GQ, Li CN, Liang ZX, Wu ZM, Jin W, et al. J Membr Sci 2006;282:450–5.
[30] Bertolucci M, Galli G, Chiellini E, Wynne KJ. Macromolecules 2004;37:3666–72.
[31] Kim DK, Lee SB, Doh KS. J Colloid Interface Sci 1998;205:417–22.
[32] Kim DK, Lee SB. J Colloid Interface Sci 2002;247:490–3.
[33] Darras V, Fichet O, Perrot F, Boileau S, Teyssié D. Polymer 2007;48: 687–95.
[34] Pusch J, Herk AMV. Macromolecules 2005;38:6909–14.
[35] Dreher WR, Jarrett WL, Urban MW. Macromolecules 2005;38: 2205–12.
[36] Alagar M, Abdul Majeed SM, Selvaganapathi A, Gnanasundaram P. Eur Polym J 2006;42:336–47.
[37] Kassis CM, Steehler JK, Betts DE, Guan Z, Romack TJ, DeSimone JM, et al. Macromolecules 1996;29(9):3247–54.
[38] Dreher WR, Singh A, Urban MW. Macromolecules 2005;38: 4666–72.
[39] Cui XJ, Zhong SL, Wang HY. Colloids Surf A 2007;303:173–8.
[40] Lin M, Chu F, Guyot A, Putaux JL, Bourgeat-Lami E. Polymer 2005;46:1331–7.